

Paclitaxel binding to the fatty acid-induced conformation of human serum albumin—Automated docking studies

Krisztina Paal* and Aliaksei Shkarupin

Faculty of Science, University of Ontario Institute of Technology, 2000 Simcoe Street North, Oshawa, Ont., Canada L1H 7K4

Received 28 June 2007; revised 5 September 2007; accepted 7 September 2007

Available online 12 September 2007

Abstract—Paclitaxel (Taxol®) binding to the conformation of human serum albumin assumed in the presence of long-chain fatty acids was studied by automated docking. Reduced binding affinities at both the primary and secondary sites were predicted, compared to those characterizing the interaction with the fatty acid-free protein. The baccatin core of paclitaxel was found to play a more important role than its C13 side chain in determining the ligand binding mode as well as in contributing to the overall binding energy at the primary site.

© 2007 Elsevier Ltd. All rights reserved.

1. Introduction

We recently reported on the high-affinity binding of the very potent anticancer agent paclitaxel (**1**, Fig. 1) to the fatty acid-free conformation of human serum albumin (HSA).¹ We located the primary and the secondary drug binding sites at the interface of subdomains IIA and IIIA, and in the cleft between domains I and III of the protein (Fig. 2), respectively, and predicted ligand binding affinities (Table 1) by automated docking. We found that the two main structural elements of paclitaxel—the baccatin core and the C13 side chain—contribute nearly equally to the binding energy at the primary site, while the ligand binding mode is dictated by the C13 side chain.

Human serum albumin,^{2,3} the main protein component of plasma, binds and transports a broad variety of endogenous and exogenous compounds. Long-chain fatty acids (LCFAs) are among the main physiological ligands of HSA. They are able to bind at least at seven different sites on the protein;⁴ binding to the five highest-affinity sites has been proposed to be cooperative.⁵ On average, 0.1–2 molar equivalents of long-chain fatty acids are bound by HSA in vivo; this ratio can however substantially increase under certain physiological and

pathological conditions.⁶ LCFA binding to albumin induces considerable conformational changes⁷ and has been shown to influence drug binding properties of the protein through direct competition and allosteric interactions.^{8–13} Thus, for a thorough understanding of the pharmacokinetic behavior of any drug known to interact with and be transported by HSA, it is imperative to be aware of any changes in binding characteristics caused by the presence of LCFA in plasma. The present article discusses the results of a computational study on the differences of paclitaxel binding to two distinct conformations of albumin: the fatty acid-free (HSA) and the fatty acid-induced (FA-HSA) conformations. In particular, changes in binding affinity, binding mode, and binding mechanism were investigated.

2. Results and discussion

The ligand molecules (Fig. 1) were docked into the two regions of FA-HSA that were identified as the primary and secondary binding sites for paclitaxel on the fatty acid-free conformation of albumin. The parameters were identical to those of our previous experiments with HSA¹ and are briefly summarized in Section 4.

The primary paclitaxel site on FA-HSA (Figs. 3 and 4) is formed by parts of subdomains IIA (helices 1 and 2 of domain II) and IIIA (helices 3 and 4 of domain III), the polypeptide strand connecting subdomains IIA and IIB, with a relatively small contribution from subdomain IIB (loop between helices 8 and 9 of domain II).

Keywords: Automated docking; Human serum albumin; Paclitaxel; Long-chain fatty acid.

* Corresponding author. Tel.: +1 905 721 8668x2939; fax: +1 905 721 3304; e-mail: krisztina.paal@uoit.ca

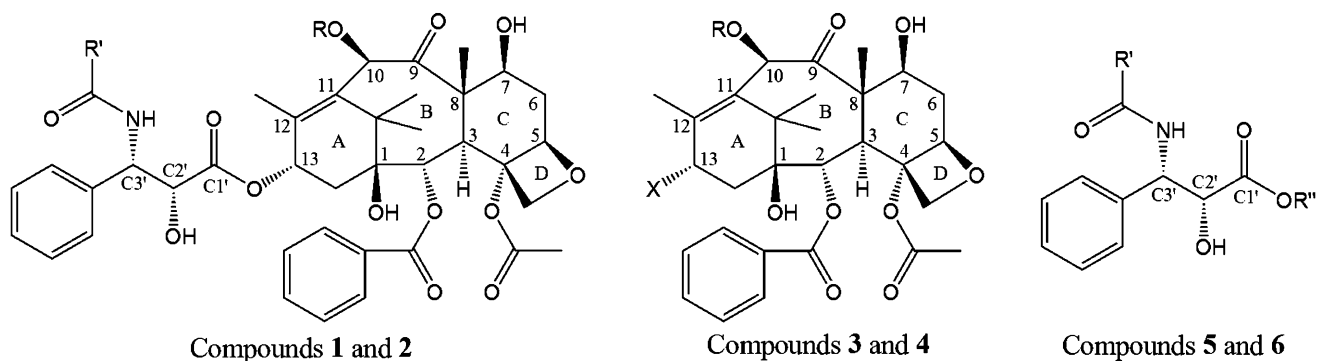


Figure 1. The ligand molecules: paclitaxel (1): $R = \text{CH}_3\text{CO}$, $R' = \text{C}_6\text{H}_5$ (phenyl); docetaxel (2): $R = \text{H}$, $R' = (\text{CH}_3)_3\text{CO}$; baccatin III (3): $R = \text{CH}_3\text{CO}$, $X = \text{OH}$; 13-deoxybaccatin (4): $R = \text{CH}_3\text{CO}$, $X = \text{H}$; C13 side chain of paclitaxel (5): $R' = \text{C}_6\text{H}_5$ (phenyl), $R'' = \text{H}$; C13 side chain of paclitaxel, methylated (6): $R' = \text{C}_6\text{H}_5$ (phenyl), $R'' = \text{CH}_3$.

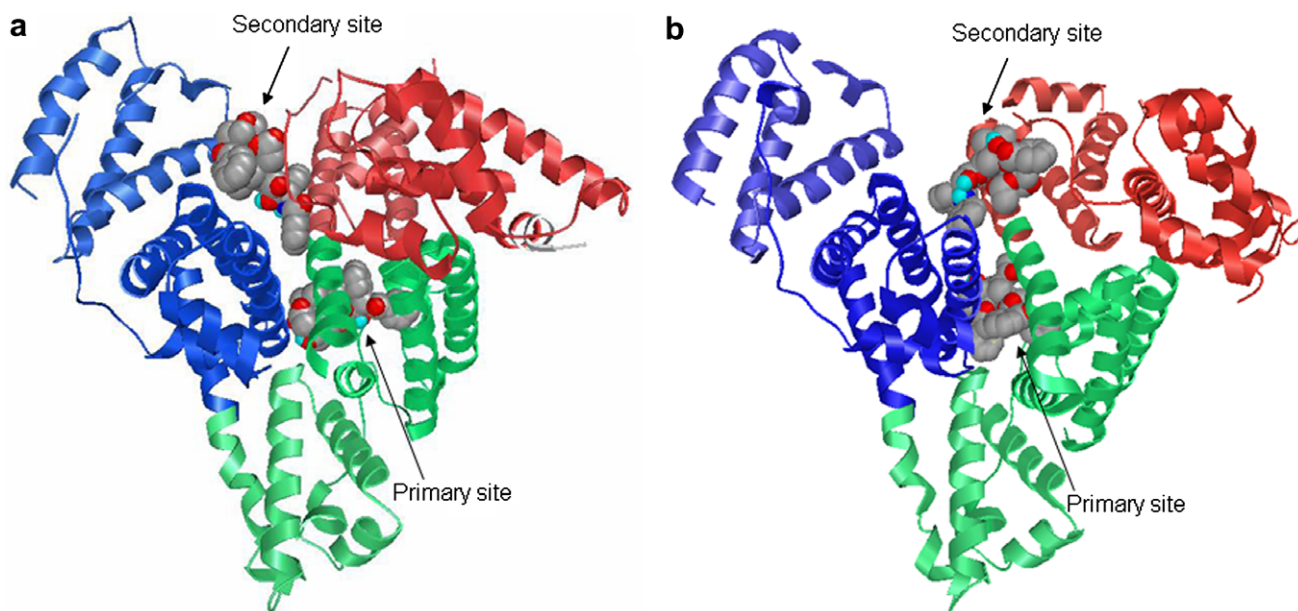


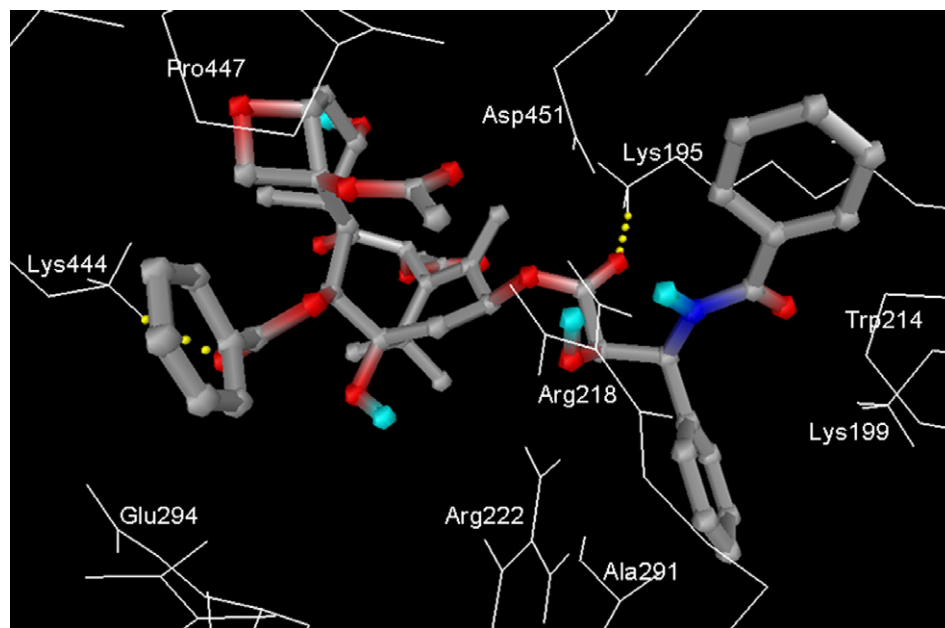
Figure 2. The primary and secondary paclitaxel binding sites on human serum albumin. (a) HSA (from PDB 1AO6), (b) FA-HSA (from PDB 1E7H). The protein domains are colored as follows: I, red; II, green; III, blue. The paclitaxel molecules (preferred conformations) are shown in a space-filling representation and are colored by atom type (carbon, grey; oxygen, red; nitrogen, blue).

Similarly to the paclitaxel–HSA complex, the baccatin core of the ligand is located at the interface of subdomains IIA and IIIA, and the C13 side chain interacts with amino acid residues of a binding pocket in subdomain IIA (commonly referred to as drug binding site I¹⁴). In comparison to its preferred conformation on HSA, paclitaxel at its primary binding site on FA-HSA (Fig. 3) is rotated by approximately 120° about an axis going through the center of ring B, causing the C2-benzoate moiety to point downward (Fig. 4). In addition, the ligand is slightly rotated about a vertical axis, presumably to allow the C13 side chain to access site I. As a result, the bottom of the cup formed by rings A–C is oriented toward the solvent instead of subdomain IIIA. Overall, paclitaxel appears to have comparable interactions with subdomain IIIA of HSA and FA-HSA, whereas interactions with subdomain IIA of the fatty acid-induced conformation are somewhat less extensive. This can mostly be attributed to the fact that

the C13 side chain of paclitaxel is not as deeply inserted into site I of FA-HSA as it is in the fatty acid-free conformation of the protein, likely caused by a 1.31-Å decrease in the distance between two of the amino acid residues (Lys195 and Arg218) that act as ‘gatekeepers’ at the entrance to the binding pocket. Moreover, by moving from the side toward the interior of the pocket and also closer to its entrance, the Arg218 residue is in an excellent position to interact with all three aromatic rings of paclitaxel to some extent and thereby to prevent the ligand from moving deeper into site I. In addition, Lys195 makes a hydrogen bond with $\text{C1}'=\text{O}$, this is also likely to help fix the ligand in its position. In contrast to the binding to HSA, where hydrogen bond interactions play an important role, only two hydrogen bonds were identified in the complex with FA-HSA (Fig. 3 and Table 2), the second one between Lys444 of subdomain IIIA and the carbonyl O of the C2-benzoate moiety. The latter also interacts with Pro447 (subdomain IIIA) and

Table 1. Ligand binding energies (kcal/mol) at the primary and secondary paclitaxel binding sites on HSA and FA-HSA

Ligand	HSA ^c		FA-HSA	
	1° site	2° site	1° site	2° site
Paclitaxel (1)				
Conformation A ^a	−11.23	−7.25	−9.78 ^c	−5.63
Lowest binding energy conformation ^b	—	—	—	−7.10 ^c
Docetaxel (2)				
Conformation A	−11.49	−5.11	−7.95	−4.56
Lowest binding energy conformation	−11.56 ^c	−7.83 ^c	−10.43	−5.43
Baccatin III (3)				
Conformation A	−8.19	−7.05	−9.16	−6.80
Lowest binding energy conformation	—	−8.17	—	−7.35
Conformation B ^d	−6.01	N.A.	−6.45	N.A.
Conformations A and B in the same cluster?	No		No	
13-Deoxybaccatin III (4)				
Conformation A	−8.06	N.A.	−9.81	N.A.
Conformation B	−6.45	N.A.	−6.00	N.A.
Conformations A and B in the same cluster?	No		No	
C13 side chain of paclitaxel (5)				
Conformation A	−9.18	N.A.	−8.25	N.A.
Conformation B	−9.08	N.A.	−6.16	N.A.
Conformations A and B in the same cluster?	Yes		No	
C13 side chain of paclitaxel, methylated (6)				
Conformation A	−7.81	N.A.	−7.32	N.A.
Conformation B	−7.24	N.A.	−5.54	N.A.
Conformations A and B in the same cluster?	Yes		No	

^a Preferred conformation as defined in Section 4.^b If different from the preferred conformation.^c 2 × 250 GA runs performed.^d Conformation showing the best overlap with the corresponding fragment of paclitaxel at its primary site on HSA or FA-HSA.^e Previously published results.¹**Figure 3.** Paclitaxel (1) binding at its primary site on FA-HSA. Hydrogen bonds are shown as yellow spheres.

amino acid side chains of subdomain IIA (Arg218, Arg222, Glu294, and Asn295). The C3′–Ph group is positioned between the positively charged side chains of Lys199 and Arg222 (π –cation interactions); it also

interacts with Arg218 and makes hydrophobic contact with Ala291. (This phenyl ring is located much deeper in site I of the fatty acid-free protein (Fig. 4), between Lys195 and Arg257.) The C3′–NHCOPh group, located

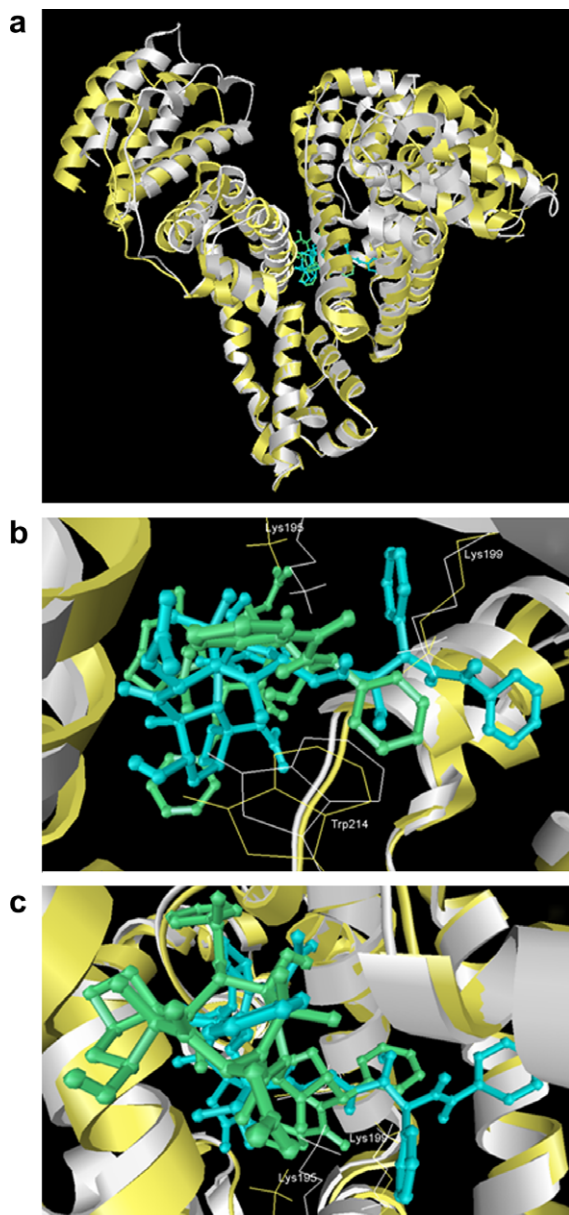


Figure 4. Superposition of paclitaxel (1) bound to its primary site on HSA (protein and ligand are colored white and blue, respectively) and FA-HSA (protein and ligand are colored yellow and green, respectively). The root-mean-square deviation between HSA and FA-HSA is 1.36 Å for the backbone atoms. (a) Front view. (b) Front view, enlarged. (c) Top view, enlarged. Prepared in Swiss-PdbViewer 3.7.

at the interface of subdomains IIA and IIIA, interacts with Lys195 (H bond), Lys199, Arg218, the edge of the Trp214 indole ring, as well as Glu450, Asp451, and Ser454. In the paclitaxel–HSA complex this phenyl ring is pinned between Leu238 and Ala291, a common position for planar rings of site I ligands.¹⁵ However, the C13 side chain of paclitaxel does not reach deep enough into site I of the fatty acid-induced conformation of albumin for any of its aromatic rings to be positioned between these two amino acid side chains. Relatively long phenyl-to-phenyl ring distances (C2–OCOPh to C3′–Ph: 11.0 Å, C2–OCOPh to C3′–NHCOPh: 11.4 Å) are maintained in the preferred paclitaxel conformation

at its primary site on FA-HSA, as seen previously for binding to HSA¹ and to tubulin,¹⁶ further stressing the importance of these aromatic functional groups in interactions with proteins. Close proximity of a pair of the aromatic rings—as observed in both polar and non-polar solvents, and referred to as hydrophobic collapse¹⁷—would indicate intramolecular interactions as opposed to interactions with the surrounding environment.

Docetaxel (2, Fig. 1) occupies the same region as paclitaxel at the primary binding site on FA-HSA (Fig. 5), with the rigid core ring system located at the interface of subdomains IIA and IIIA and the C13 side chain reaching into the binding pocket in subdomain IIA. Four hydrogen bond interactions were identified, two between substituents of the core ring system and amino acid residues of subdomain IIIA and two between functional groups of the C13 side chain and amino acid residues of subdomain IIA (Fig. 5 and Table 2). The C3′–Ph group is positioned between helices 1 and 6 of domain II and is surrounded by several charged amino acid residues (Lys195, Lys199, His288, and Glu292). The C3′–NHCOO[−]Bu moiety is located in the area defined by helices 1, 2, and 6 of domain II and interacts with the side chains of Lys199, Arg218, Arg222, Leu238, His242, Arg257, and Ala291. The aromatic ring of the C2-benzoate functionality is positioned between the helix shared by domains I and II (helix 10 of domain I continuing as helix 1 of domain II) and helices 3 and 4 of domain III, in close proximity to the side chains of Glu188, Lys195, Lys436, Asp451, and Tyr452. This group is pinned between Pro339 and His440 at the primary site on HSA, a position that is not accessible for the C2–OCOPh moiety in the complex of docetaxel with FA-HSA: this functional group points upward due to rotation of the ligand. The bottom of the cup formed by rings A–C is protected from the bulk solvent by amino acid residues of helices 3 and 4 of domain III (subdomain IIIA).

Baccatin III (3, Fig. 1) resides at the interface of domains II and III, occupying the same region as the ring system of paclitaxel (Fig. 6). It is however rotated by 180° about an axis going through the center of ring B, causing the C2-benzoate and C10-acetate groups to switch positions. Baccatin III was found to make five hydrogen bond interactions with FA-HSA at this site (Table 2). This may very well be the explanation for no substantial decrease in binding affinity in comparison to paclitaxel as might be expected due to the absence of the C13 side chain, as is indeed the case for binding to HSA. Lack of the favorable interactions between the paclitaxel C13 side chain and subdomain IIA appears to be compensated by three additional H bonds made by baccatin III in comparison to paclitaxel, two of which are contributed by the C13–OH group itself (Table 2). The aromatic ring of the C2–OCOPh moiety is perfectly situated for interactions with amino acid residues of both domains II (Glu188, Lys195, and Glu292) and III (Asp451 and Tyr452). The bottom of the cups formed by rings A–C is oriented toward the solvent but is shielded from the bulk of the solvent by surface residues of the protein.

Table 2. Hydrogen bond interactions between ligand molecules and amino acid residues at the primary and secondary paclitaxel binding sites on FA-HSA

Ligand ^a	Primary site			Secondary site		
	Donor	Acceptor	Distance (Å)	Donor	Acceptor	Distance (Å)
1	Lys444	O=C (C2–O–CO–)	1.9	<i>No H bonds at this site</i>		
	Lys195	O=C1'	1.8			
2	C1–OH	Asp451	2.1	Arg114	O–C1	1.9
	Lys444	O–C7	1.7	Arg117	O=C (C4–O–CO–)	2.1
	Arg222	O–C2'	2.2			
	N–H	Ala291 (C=O, bb ^b)	2.0			
3	Arg218	O–C13	2.1	<i>No H bonds at this site</i>		
	Arg218	O–C13	1.7			
	Arg222	O–C4	2.2			
	C7–OH	Val293 (C=O, bb)	2.2			
	Lys444	O=C9	1.9			

^a Ligands are as shown in Figure 1: paclitaxel (1), docetaxel (2), baccatin III (3).

^b bb, Backbone; sc, side chain; the side chain functional group of the amino acid residue is involved, unless otherwise noted.

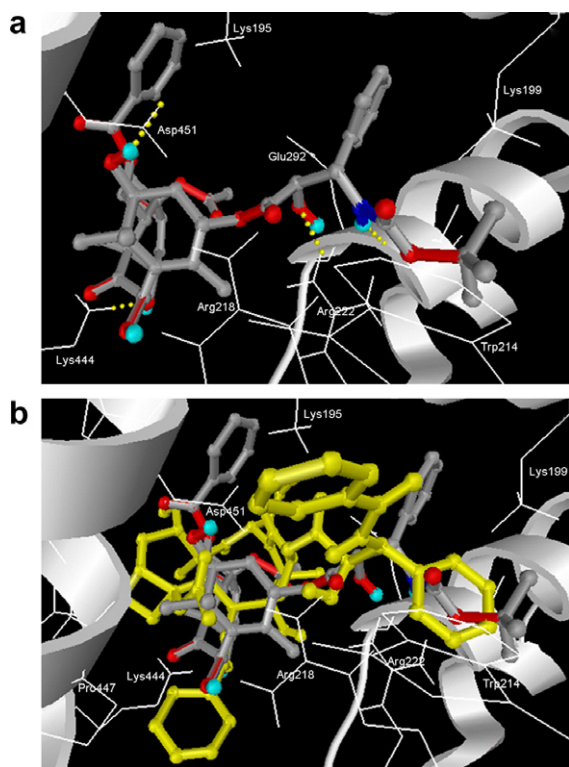


Figure 5. Preferred conformation of docetaxel (2) at the primary paclitaxel binding site on FA-HSA. (a) Docetaxel alone; hydrogen bonds are shown as yellow spheres. (b) Superposition with paclitaxel (1, yellow).

To better understand the binding mode of paclitaxel at its primary site on the fatty acid-induced conformation of albumin, its C13 side chain (5, Fig. 1) was docked into the same site as a separate entity. The preferred conformation of this ligand shows excellent overlap with the corresponding fragment of paclitaxel at the primary site on HSA.¹ Thus, we were initially surprised to learn that the C13 side chain binds relatively deep in site I of FA-

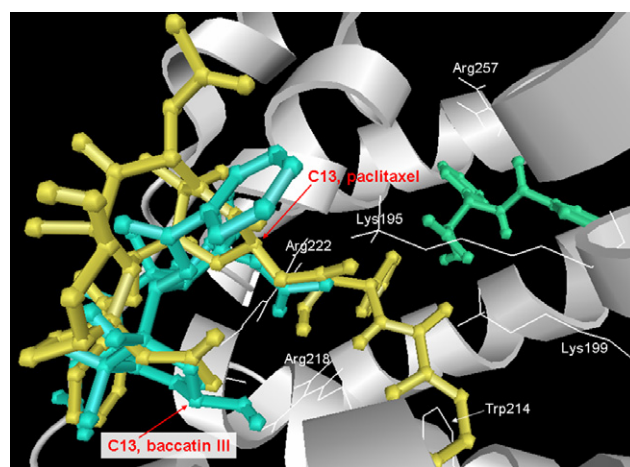


Figure 6. Preferred ligand conformations at the primary paclitaxel binding site on FA-HSA. Paclitaxel (1), yellow; baccatin III (3), blue; C13 side chain of paclitaxel (5), green.

HSA, at a location that is distinct from that occupied by the corresponding fragment of paclitaxel (Fig. 6). However, upon closer examination of the complex it became quite clear why this position is favored by the C13 side chain as a stand-alone ligand. Its preferred binding mode allows both aromatic groups to participate in π -cation interactions: the C3'–Ph ring interacts with Arg257 and the phenyl ring of C3'–NHCOPh with His242 (the latter two rings are nearly parallel). Interestingly, neither of the planar groups of 5 is located between Leu238 and Ala291 as might be anticipated. This ligand orientation however allows favorable ionic interactions of the C1'–carboxylate moiety with the positively charged residues of Lys199 and Arg222. In addition, three hydrogen bonds are formed, two with Arg257 and one with His242 as donors (Table 3). Thus, in contrast to its interaction with the fatty acid-free conformation of albumin, where the C13 side chain determined the paclitaxel binding mode, at the primary site on

Table 3. Hydrogen bond interactions between fragments of paclitaxel and amino acid residues at the primary paclitaxel binding site on FA-HSA

Ligand ^a	Donor	Acceptor	Distance (Å)	Conformation ^b
3 ^c				
4				
	Lys444	O=C (C4–O–CO–)	2.0	A
	C7–OH	Pro447 (C=O, bb ^d)	2.1	A
	Arg218	O–C7	2.0	A
	Arg218	O–C7	2.1	A
	Arg222	O=C9	1.7	A
	Arg222	O–C10	2.2	A
	Asn295	O=C (C10–O–CO–)	2.0	A
	C7–OH	Tyr452	2.1	B
	Lys444	O=C (C2–O–CO–)	1.8	B
5				
	Arg257	O=C (C3'–NHCO–)	2.0	A
	Arg257	O=C (C3'–NHCO–)	2.1	A
	His242	O–C2'	1.8	A
	Arg222	[–] O ₂ C1'	1.8	B
6				
	Arg222	O–C1'	2.1	B

^a Ligands are as shown in Figure 1: baccatin III (3), 13-deoxybaccatin (4), C13 side chain of paclitaxel (5), C13 side chain of paclitaxel, methylated (6).

^b Ligand conformations A and B as defined in Table 1.

^c Hydrogen bonds of conformation A are listed in Table 2, conformation B makes no hydrogen bonds with FA-HSA.

^d bb, backbone; sc, side chain; the side chain functional group of the amino acid residue is involved, unless otherwise noted.

FA-HSA, it is the baccatin core of this ligand that plays the more important role in this respect. Though it only dictates the location and not the specific orientation of binding as illustrated by Figure 6. The most likely explanation for the distinct binding mechanisms of paclitaxel to the two different conformations of albumin is the movement of some of the amino acid side chains within site I as a result of long-chain fatty acid binding, most notably those of Lys195 and Arg218 as discussed in detail in the second paragraph of this Section.

Paclitaxel and docetaxel have been found to bind with decreased affinity to the primary paclitaxel site on FA-HSA, whereas baccatin III interacts somewhat more strongly with the fatty acid-induced than it does with the fatty acid-free conformation (Table 1). Lower binding affinity of paclitaxel for the former can be explained by a smaller number of hydrogen bond interactions, as well as somewhat greater solvent exposure of the ligand. However, it is not straightforward to account for the reduced binding affinity of docetaxel, as the number of hydrogen bond interactions did not decrease significantly and the extent of ligand–protein interactions in the complexes with HSA and FA-HSA appears comparable.

To dissect the contributions of its two main structural elements to the binding energy, modified fragments of paclitaxel (4 and 6, Fig. 1) were docked into the primary binding site as stand-alone ligands. Rationales for the deletion of the C13–OH of baccatin and for the methylation of the C13 side chain have been described elsewhere.¹ Similarly to our previous studies with the fatty acid-free conformation of albumin, we found that the baccatin core and the C13 side chain contribute approximately equally to the overall binding energy at the pri-

mary paclitaxel binding site on FA-HSA (Table 1). However, the relative importance of the two fragments appears to have changed, the rigid core ring system is the somewhat more important contributor in the complex with FA-HSA (Fig. 7). Figure 7 also demonstrates that the reduced binding affinity of paclitaxel for the fatty acid-induced conformation of HSA is mainly the result of a decrease in the binding affinity of its C13 side chain.

The secondary paclitaxel binding site on FA-HSA is located in the cleft between domains I and III (Fig. 2b). The rigid core ring system of the ligand interacts with helix 10 of domain I (subdomain IB) and the polypeptide strand connecting subdomains IA and IB, whereas the C13 side chain faces helices 3 and 4 of domain III (subdomain IIIA). The orientation is quite different from that at the same site on HSA, where it is the bot-

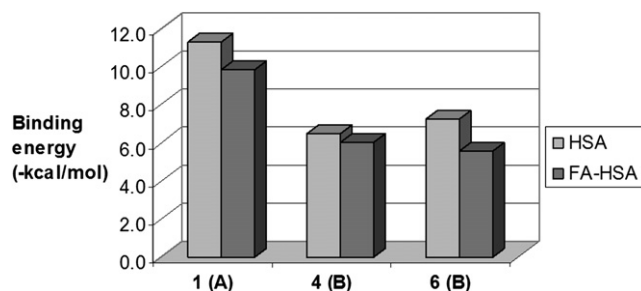


Figure 7. Changes in ligand binding energies at the primary paclitaxel site on HSA and FA-HSA. Ligands are as shown in Figure 1: paclitaxel (1), 13-deoxybaccatin (4), C13 side chain of paclitaxel, methylated (6). Ligand conformations A and B are as defined in Table 1.

tom of the cup formed by rings A–C that faces and interacts with subdomain IIIA and the C13 side chain is oriented toward domain I of the protein (Fig. 2a). The significant change in ligand orientation at this site is not surprising, considering that this is the region that is most affected by the binding of long-chain fatty acids to albumin: the cleft between domains I and III opens up as a result of rotations of each of these two domains relative to domain II.⁷ It is also interesting to note that baccatin III shows reasonable overlap with the corresponding fragment of paclitaxel at its secondary site on FA-HSA (vide infra); thus, it appears that this is a favorable position for the rigid core ring system. The C3'–Ph group is surrounded by residues of subdomain IIIA (Glu425, Arg428, Asn429, and Lys432), Lys519 of subdomain IIIB, as well as residues of subdomain IB (Arg186, Asp187, Lys190). The C3'–NHCOPh functionality is in close proximity to Asn429, Gln459, Leu463 (subdomain IIIA), and Arg197. The third aromatic ring (C2–OCOPh) interacts with the strand connecting the two subdomains of domain I as well as with residues of helix 8 of domain I (Arg145, His146; subdomain IB). No hydrogen bond interactions between paclitaxel and FA-HSA were identified at this site.

The orientation of docetaxel at the secondary site on FA-HSA is different from that of paclitaxel: it is the bottom of the cup formed by rings A–C that faces domain III; however the distance is too great for considerable attractive forces to operate. The C13 side chain interacts with the strand connecting subdomains IA and IB as well as with helix 10 of domain I. The C2-benzoate group points upward and participates in a π -cation interaction with Arg114. Two hydrogen bonds were identified with Arg114 and Arg117 as donors (Table 2).

Baccatin III at its secondary site on FA-HSA resides between the polypeptide strand connecting subdomains IA and IB and helix 10 of domain I. The bottom of the cup formed by rings A–C faces the strand between the two subdomains of domain I and the phenyl ring of the C2-benzoate group points downward, with one side facing helix 8 of domain I and the other side facing the cleft between domains I and III. No hydrogen bonds were identified between baccatin III and FA-HSA at this site, in contrast to the secondary binding site on HSA.

Thus far the pure effects of the fatty acid-induced *conformational changes* of human serum albumin on taxane binding characteristics have been discussed. To obtain a more complete picture of how the presence of LCFAs in plasma may alter drug binding, the potential for direct competition also needs to be considered. LCFA site 7⁴ overlaps with the primary paclitaxel binding site on FA-HSA to a very small extent: the end of the hydrophobic tail of the fatty acid anion and the C13 side chain of paclitaxel or docetaxel would collide should these ligands bind simultaneously. However, LCFA site 7 appears to be a low-affinity site¹³ that is not likely to be occupied under normal physiological conditions; direct competition with paclitaxel or docetaxel at this site should only be expected if the LCFA-to-albumin molar ratio in plasma exceeds five. Indeed, *decreased* binding

at a LCFA-to-albumin ratio of six and *increased* binding at a LCFA-to-albumin ratio of not greater than four have been reported for some site I drugs (warfarin, phenprocoumon,¹¹ and furosemide¹²). While the latter effect is most likely the result of allosteric interactions, the former is presumably caused by direct competition, considering the high degree of overlap between the primary warfarin site¹⁸ (PDB IDs 1H9Z and 1HA2) and LCFA site 7. Competition of LCFA with paclitaxel or docetaxel, should it occur, is expected to be considerably weaker due to the much smaller degree of overlap between the respective binding sites.

The secondary paclitaxel binding site on FA-HSA is very close to LCFA site 1,^{7,13} another relatively low-affinity site, which—contrary to LCFA site 7—is occupied under normal physiological conditions in 2–40% of the albumin molecules if LCFA binding is indeed cooperative as proposed.⁵ The carbonyl O of the C10-acetate of paclitaxel bound at the secondary site on FA-HSA is about 1.5 Å away from one of the carboxylate oxygens of the fatty acid anion bound at LCFA site 1, close enough for unfavorable electrostatic repulsions. Though this may be reduced by rotation about the C10–O bond it is likely to result in decreased binding affinity of one or both of the ligands in the presence of the other. On the other hand, the same O atom of the fatty acid anion is close enough to the C7–OH of paclitaxel to make a H bond (the other O of the carboxylate moiety is H bonded to Arg117), which may result in synergistic binding. Similar considerations apply to baccatin III. The C3'–Ph group of docetaxel bound at the secondary site is about 2 Å away from the fatty acid anion bound at LCFA site 1, likely to cause unfavorable van der Waals repulsions between the two ligands, this however might be minimized by rearrangement of the C13 side chain conformation. It is interesting to note that the carbonyl O of the C4-acetate of docetaxel makes a H bond with Arg117, which in turn is H bonded to the fatty acid carboxylate.

3. Conclusion

Both paclitaxel and docetaxel were predicted to bind with reduced affinity at their primary and secondary sites on FA-HSA in comparison to HSA. Contrary to the interaction with the fatty acid-free conformation of albumin, it is the baccatin core of paclitaxel that plays the more important role in binding at the primary site on FA-HSA: it determines the location—though not the precise orientation—of the ligand and its relative contribution to the overall binding energy is increased. These changes can largely be attributed to the movements of individual amino acid side chains at the binding site in the presence of bound LCFAs. The primary paclitaxel binding site slightly overlaps with LCFA site 7, direct competition with LCFA is thus in principle possible. This is however unlikely to occur in vivo given the plasma fatty acid levels observed under a variety of normal and pathological conditions and the low affinity of LCFA site 7. The predicted binding energies at the primary paclitaxel site can be considered valid at LCFA-to-albumin ratios not exceeding five. On the other hand,

paclitaxel and docetaxel binding affinities at the secondary site are very likely to be influenced by fatty acids bound at LCFA site 1.

4. Methods

Version 3.0.5 of AutoDock^{19–21} was used for the docking studies. Ligand files were prepared as previously described.¹ The HSA X-ray crystal structure 1E7H was utilized for the docking experiments. All water and palmitic acid molecules were removed and Swiss-PdbViewer 3.7 was used to repair the PDB file. Grid maps of 90 × 90 × 90 points with a grid-point spacing of 0.375 Å were generated using the AutoGrid tool. The maps were centered on His242 (HE2[†]) and Arg114 (HH22[†]) for the primary and the secondary binding sites of paclitaxel, respectively. Two hundred and fifty Genetic Algorithm (GA) runs were performed with parameters identical to those used in previous studies on HSA.¹ Cluster analysis of the resulting conformations was performed as previously described.¹ Briefly, clusters were ranked in order of increasing binding energy of the lowest binding energy conformation in each cluster. The most populated of the first five clusters was selected for further analysis;²² the lowest binding energy conformation of this cluster is referred to as the preferred conformation and is described in Section 2.

Acknowledgments

The authors greatly appreciate the invaluable technical assistance of Drs. Thomas Hu and Ken Pu.

References and notes

1. Paal, K.; Shkarupin, A.; Beckford, L. *Bioorg. Med. Chem.* **2007**, *15*, 1323–1329.
2. Peters, T. J. *All About Albumin: Biochemistry, Genetics, and Medical Applications*; Academic Press: San Diego CA, 1996.
3. Carter, D. C.; Ho, J. X. *Adv. Protein Chem.* **1994**, *45*, 153–203.
4. Bhattacharya, A. A.; Grune, T.; Curry, S. *J. Mol. Biol.* **2000**, *303*, 721–732.
5. Fang, Y. N.; Tong, G. C.; Means, G. E. *Biochim. Biophys. Acta* **2006**, *1764*, 285–291.
6. Naranjo, C. A.; Sellers, E. M. In *Drug–Protein Binding*; Reidenberg, M. M., Erill, S., Eds.; Praeger Scientific: New York, 1986; pp 233–251.
7. Curry, S.; Mandelkow, H.; Brick, P.; Franks, N. *Nat. Struct. Biol.* **1998**, *5*, 827–835.
8. Colombo, R.; Pinelli, A. *Pharmacology* **1982**, *25*, 73–81.
9. Menke, G.; Worner, W.; Kratzer, W.; Rietbrock, N. *Naunyn Schmiedeberg's Arch. Pharmacol.* **1989**, *339*, 42–47.
10. Worner, W.; Preissner, A.; Rietbrock, N. *Eur. J. Clin. Pharmacol.* **1992**, *43*, 97–100.
11. Vorum, H.; Honore, B. *J. Pharm. Pharmacol.* **1996**, *48*, 870–875.
12. Takamura, N.; Shinozawa, S.; Maruyama, T.; Suenaga, A.; Otagiri, M. *Biol. Pharm. Bull.* **1998**, *21*, 174–176.
13. Simard, J. R.; Zunszain, P. A.; Hamilton, J. A.; Curry, S. *J. Mol. Biol.* **2006**, *361*, 336–351.
14. Sudlow, G.; Birkett, D. J.; Wade, D. N. *Mol. Pharmacol.* **1976**, *12*, 1052–1061.
15. Ghuman, J.; Zunszain, P. A.; Petitpas, I.; Bhattacharya, A. A.; Otagiri, M.; Curry, S. *J. Mol. Biol.* **2005**, *353*, 38–52.
16. Lowe, J.; Li, H.; Downing, K. H.; Nogales, E. *J. Mol. Biol.* **2001**, *313*, 1045–1057.
17. Jimenez-Barbero, J.; Amat-Guerri, F.; Snyder, J. P. *Curr. Med. Chem. Anti-Cancer Agents* **2002**, *2*, 91–122.
18. Petitpas, I.; Bhattacharya, A. A.; Twine, S.; East, M.; Curry, S. *J. Biol. Chem.* **2001**, *276*, 22804–22809.
19. Goodsell, D. S.; Olson, A. J. *Proteins* **1990**, *8*, 195–202.
20. Morris, G. M.; Goodsell, D. S.; Huey, R.; Olson, A. J. *J. Comput. Aided Mol. Des.* **1996**, *10*, 293–304.
21. Morris, G. M.; Goodsell, D. S.; Halliday, R. S.; Huey, R.; Hart, W. E.; Belew, R. K.; Olson, A. J. *J. Comput. Chem.* **1998**, *19*, 1639–1662.
22. Kallblad, P.; Mancera, R. L.; Todorov, N. P. *J. Med. Chem.* **2004**, *47*, 3334–3337.

[†] Atom identification used by AutoDock.